

A STUDY FOR RAPID PHASE AMBIGUITY RESOLUTION ON PRECISE KINEMATICS GPS POSITIONING

Chi-Hsiu Hsieh* and Joz Wu**

* Ph. D. candidate, Dept. of Civil Engrg., NCU. and Lecturer of C.E., Army Academy.

** Prof. and Director, Ctr. for Space and Remote Sensing Res., Nat. Central Univ.

R3-417, CSRSR, National Central University, Jhongli 320, TAIWAN, R.O.C.

Tel: 886-3-4227151 ext 57615, Fax: 886-3-4254908

E-mail: jieshio.hsieh@msa.hinet.net; jozwu@csrsr.ncu.edu.tw

KEY WORDS: Variance components; Decorrelating transformation; Ambiguity resolution.

ABSTRACT: The GPS has become a usable and valuable means on precise kinematics positioning in recent years. An accuracy of centimeter level (standard deviation) or even better resolution can be reached over the short baselines; nevertheless, a reference station needs to be established in the vicinity of the roving antenna to appropriately reduce error sources. The key to precise kinematics GPS positioning is the carrier-phase integer ambiguity resolution. Over short distances (<10 km, depending on the ionospheric conditions), a common practice is to neglect the ionospheric effects. However, over longer distances, differential ionospheric residuals become larger and may hamper the phase integer ambiguity resolution process, or even make it impossible.

Therefore, the reduction of the differential ionospheric effects is one of the most important steps to improve ambiguity resolution process, and hence for the precise medium and long-range kinematic positioning. This paper presents the analyses and algorithms of the model; (a) the additional virtual DD ionospheric observation equation to the stochastics of measurement for the ionospheric parameters can be estimated, (b) the measurement covariance matrix has a positive impact on the estimated covariance matrix of the float ambiguity parameter, and (c) then transformed by using a volume-preserving diagonalization technique, whole-cycle phase integer ambiguities have been obtained efficiently, in particular for single-baseline length up to 55 km.

1. INTRODUCTION

The range between the navigation GPS (global positioning system) satellite and a user can be measured at a signal receiving epoch and process to determine the user's three-dimensional position, in either a static or an on-the-fly mode. Basically, the quality of satellite positioning depends on the precision of range measurement, the geometry of satellite, and the extent of which user equivalent range errors are removed. A stochastic range measurement is well characterized by its variance, and any two measurements by their covariance.

As expressed later, all the estimators will involve the positive definite covariance matrices. The least effort made by an analyst is by treating an initial covariance matrix as the identity matrix. A measurement that results from the low-elevation satellite signal tracking has a larger variance than that of a high-elevation satellite. An independent, identically distributed error model then represents quite a good choice for GPS positioning. In reality, there exist only prior estimates of the variance and covariance, which may lead to sub-optimal position solutions. This paper is aimed to describe a better, unbiased estimator for variance and covariance components, based on the residuals of range measurement.

2. BASIC DOUBLE-DIFFERENCE OBSERVATION MODELS

The basic four double-difference observation equations of the carrier phase $\Delta\nabla\Phi_1, \Delta\nabla\Phi_2$ (m) and the pseudorange $\Delta\nabla\rho_1, \Delta\nabla\rho_2$ (m) can be written as:

$$\Delta\nabla\Phi_1 = \lambda_1\Delta\nabla\varphi_1 = \Delta\nabla R + \Delta\nabla T_{\text{trop}} - \Delta\nabla I - \lambda_1\Delta\nabla N_1 + \Delta\nabla\varepsilon_{1,\Phi_1}$$

$$\begin{aligned}
\Delta\nabla\Phi_2 &= \lambda_2\Delta\nabla\phi_2 = \Delta\nabla R + \Delta\nabla T_{\text{trop}} - \alpha_f\Delta\nabla I - \lambda_2\Delta\nabla N_2 + \Delta\nabla\varepsilon_{2,\Phi_2} \\
\Delta\nabla\rho_1 &= \Delta\nabla R + \Delta\nabla T_{\text{trop}} + \Delta\nabla I + \Delta\nabla\varepsilon_{3,\rho_1} \\
\Delta\nabla\rho_2 &= \Delta\nabla R + \Delta\nabla T_{\text{trop}} + \alpha_f\Delta\nabla I + \Delta\nabla\varepsilon_{4,\rho_2}
\end{aligned} \tag{1}$$

where the reference receiver is denoted by the subscript i , the user receiver denoted by j . The superscript g stands for a reference satellite, h stands for another satellite, with the convention, $\Delta\nabla\rho = \rho_j^h - \rho_i^h - \rho_j^g + \rho_i^g$ and $\Delta\nabla\Phi = \Phi_j^h - \Phi_i^h - \Phi_j^g + \Phi_i^g$, etc. The stochastic, zero-mean pseudorange error and phase error are indicated by ε_ρ (m) and ε_Φ (m), respectively. The λ_1 and λ_2 (m) stand for the L1 and L2 carrier wavelength. The R (m) represents the Euclidean satellite-receiver distance. N_1 , and N_2 (cycle) denote the integer ambiguity. And $\alpha_f = 77/60$.

For over short distances (<10 km, depending on the ionospheric conditions), the ionospheric effects are neglected for common practice. An accuracy of centimeter level (standard deviation) or even better resolution can be reached. However, while in longer distances, the differential ionospheric residuals become larger and may hamper the phase integer ambiguity resolution process, or even make it impossible. Therefore, this paper presents the analyses of modeling algorithms with an additional virtual double-difference ionospheric observation equation which can estimate the ionospheric parameters of the stochastic measurement (Goad and Yang, 1997). The virtual double-difference ionospheric observation equation can be written as:

$$\begin{aligned}
m &= (\nabla\Delta I)_0 + \nabla\Delta\varepsilon_m \\
\sigma_m^2 &= \lim_{\tau \rightarrow 0} \sigma_{ij}^{2gh}(\tau, s) = \sigma_\infty^2 \cdot (1 - e^{-2s/D})
\end{aligned} \tag{2}$$

where m is a priori observation of the double-difference ionospheric equals to 0, and σ_m^2 is the variance of the ionosphere, a priori observation that the strength of the stochastic measurement is dependent on the instantaneous baseline length, and τ is the time interval, and s is the instantaneous baseline length. Assuming that σ_∞^2 equals to 2.0 m² to the upper limit of all practical kinematics GPS operations, the variance of the double-difference ionospheric effect at a distance approximately D equals to 1500 km. σ_m has the values of 0.012 m and 0.353 m in the distances of 0.115 km and 100.0 km, respectively.

3. LEAST-SQUARES ESTIMATION

A linear system of error equations is given as below,

$$\mathbf{B} \mathbf{v} + \mathbf{A} \mathbf{x} = \mathbf{l} \quad \text{with} \quad \mathbf{\Sigma} \tag{3}$$

$\begin{matrix} c \times n & n \times 1 & c \times u & u \times 1 & c \times 1 \\ & & & & n \times n \end{matrix}$

an optimal solution for the \mathbf{x} vector partly depends on the corresponding, posterior covariance matrix $\mathbf{\Sigma}_x$; by analogy, the solution of \mathbf{v} vector is the function of the matrix $\mathbf{\Sigma}_v$. The least-squares principle states that the quadratic form, $\mathbf{v}^T \mathbf{\Sigma}^{-1} \mathbf{v}$, is the minimum. According to the law of error propagation, the $(\mathbf{A}^T \mathbf{\Sigma}_l^{-1} \mathbf{A})^{-1}$ term is exactly the covariance matrix $\mathbf{\Sigma}_x$ so that

$$\mathbf{x} = \mathbf{\Sigma}_x \mathbf{A}^T \mathbf{\Sigma}_l^{-1} \mathbf{l}, \quad \text{and} \quad \mathbf{v} = \mathbf{\Sigma} \mathbf{B}^T \mathbf{k} = \mathbf{\Sigma} \mathbf{B}^T \mathbf{\Sigma}_k \mathbf{l} = \mathbf{\Sigma} \mathbf{B}^T \mathbf{\Sigma}_k \mathbf{B} \mathbf{\Sigma} \mathbf{B}^T \mathbf{\Sigma}_l^{-1} \mathbf{l} = \mathbf{\Sigma}_v \mathbf{B}^T \mathbf{\Sigma}_l^{-1} \mathbf{l} \tag{4}$$

The prior measurement error covariance matrix $\mathbf{\Sigma}$ is thus most fundamental. As a rule of thumb, the precision of GPS measurement can be estimated to be one hundredth of a wavelength. The ratio of the L2-carrier phase variance to that of the L1-carrier is determined to be the quantity of $(\lambda_2/\lambda_1)^2 = (77/60)^2$, or the measurement variance (m²) results in the

expression of $V(\Phi_2) = (\lambda_2/\lambda_1)^2 V(\Phi_1)$. For the C/A- and P-code pseudoranges, their variances (m^2) can be set equal to the expressions of $V(\rho_1) = (154)^2 V(\Phi_1)$ and $V(\rho_2) = (\lambda_2/\lambda_1)^2 V(\rho_1)$, respectively.

3. VARIANCE-COMPONENT ESTIMATOR

In Eq. (3), an additional decomposition of the covariance matrix into m components is considered, $\Sigma = \sum_{i=1}^m \sigma_i^2 C_i$, where the accompanying matrix C_i each has $n \times n$ dimensions. The corresponding σ_i^2 stands for an unknown scale factor. An unbiased variance-component estimator is defined (Wu and Yeh, 2005) as follows

$$\hat{\sigma}_i^2 = \frac{\mathbf{v}^T \Sigma^{-1} C_i \Sigma^{-1} \mathbf{v}}{\text{tr}(\mathbf{B} C_i \mathbf{B}^T \Sigma_k^{-1})}, \quad i \in \{1, 2, \dots, m\} \quad (5)$$

With the new $\hat{\sigma}_i^2$ estimated by Eq. (5), a new covariance Σ matrix is given as $\sum_{i=1}^m \hat{\sigma}_i^2 C_i$. The new Σ leads to new Σ_l , Σ_k matrices and a new residual \mathbf{v} vector, which contributes to updating $\hat{\sigma}_i^2$ again. The iteration may stop when the estimator reproduces itself which means the scaling $\hat{\sigma}_i^2$ variance components all approach unity. In this study, the dual-frequency carrier phase and pseudorange are assumed to be independent and identically distributed, each accompanying, positive semidefinite matrix is diagonal. They are explicitly defined $m=3$ as follows

$$\begin{aligned} C_1 &= \text{diag}(V(\Phi_{1,i}^s), V(\Phi_{1,j}^s), V(\Phi_{2,i}^s), V(\Phi_{2,j}^s), 0, 0, 0, 0, 0, 0, V(\Phi_{1,i}^h), V(\Phi_{1,j}^h), V(\Phi_{2,i}^h), V(\Phi_{2,j}^h), 0, 0, 0, 0, 0, 0, \dots), \\ C_2 &= \text{diag}(0, 0, 0, 0, V(\rho_{1,i}^s), V(\rho_{1,j}^s), V(\rho_{2,i}^s), V(\rho_{2,j}^s), 0, 0, 0, 0, 0, 0, V(\rho_{1,i}^h), V(\rho_{1,j}^h), V(\rho_{2,i}^h), V(\rho_{2,j}^h), 0, 0, \dots), \\ C_3 &= \text{diag}(0, 0, 0, 0, 0, 0, 0, 0, 0, 0, V(m_i^s), V(m_j^s), 0, 0, 0, 0, 0, 0, 0, 0, V(m_i^h), V(m_j^h), \dots). \end{aligned}$$

4. DECORRELATING TRANSFORMATION

A covariance matrix factorization can lead to an expression of $\Sigma_a = \mathbf{U} \mathbf{D} \mathbf{U}^T$, where the matrix \mathbf{U} is an upper unit triangular matrix and \mathbf{D} is a diagonal matrix. An intU operation changes the entries of \mathbf{U} to integers. The transformed matrix such that $\bar{\Sigma}_a = (\text{int } \mathbf{U})^{-1} \Sigma_a (\text{int } \mathbf{U})^{-T}$, is thus more diagonally dominant. Alternatively, a lower triangular matrix \mathbf{L} can be replaced by the matrix \mathbf{U} . If at the k -th iteration, either $\text{int } \mathbf{U}_k$ or $\text{int } \mathbf{L}_k$ becomes an identity matrix, the definition as shown in Eq. (6) represents a decorrelating transformation (Mohamed and Schwarz, 1998).

$$\mathbf{T}^{-1} = (\text{int } \mathbf{L}_k)^{-1} (\text{int } \mathbf{U}_k)^{-1} (\text{int } \mathbf{L}_{k-1})^{-1} (\text{int } \mathbf{U}_{k-1})^{-1} \dots (\text{int } \mathbf{L}_1)^{-1} (\text{int } \mathbf{U}_1)^{-1} \quad (6)$$

The \mathbf{T}^{-1} matrix has the integer-valued element. The determinant of \mathbf{T}^{-1} is equal to one because both relationships of $\det(\text{int } \mathbf{L}_i)^{-1} = 1$ and $\det(\text{int } \mathbf{U}_i)^{-1} = 1$ are true. This makes the transformation matrix [Eq. (6)] be a volume-preserving (Teunissen et al., 1997). The ambiguity vector \mathbf{a} and the covariance matrix Σ_a are mapped into Eq. (7) such as

$$\boldsymbol{\alpha} = \mathbf{T}^{-1} \mathbf{a} \quad \text{and} \quad \Sigma_{\boldsymbol{\alpha}} = \mathbf{T}^{-1} \Sigma_a \mathbf{T}^{-T} \quad (7)$$

Geometrically centered at $\boldsymbol{\alpha}$, the new $\Sigma_{\boldsymbol{\alpha}}$ (hyper-)ellipsoid will appear spheroidal due to diagonal dominance. Some vectors $\text{int}(\boldsymbol{\alpha})$ are chosen and transformed back in terms of $\mathbf{T} \text{int}(\boldsymbol{\alpha})$, each resulting in a potential, integer-valued \mathbf{a} ambiguity solution. Based on the \mathbf{a} ambiguity determination, Eqs. (4) are then obtained the position and residual solutions.

5. NUMERICAL POSITIONING TESTS

The computer program, called ManGo, has been developed by using the previous sections were tested on three sets of GPS observations. The data of observations were from the north of Taiwan permanent GPS network as shown Fig. 1 at A.M. 10~11, DOY 245 of 2005: (i) the CSRF using a dual-frequency Leica GPS SR530 receiver and LEIAT 504 antenna at Hsin-tien of Taipei, (ii) the SINP using a dual-frequency Leica SR530 receiver and 502 antenna at St. John's University (Tam-sui of Taipei), and (iii) the LANY using a dual-frequency Leica GPS SR530 receiver and LEIAT 504 antenna at Lan-Yang Ins. of Technology (Tou-chen of Ilan). The parameters of GPS receiver setting indicated a 1.0 Hz sampling rate, a 15° tracking mask angle, and carrier-smoothed ranging. Seven to nine GPS satellites were very often in view. The satellite orbit has been the IGS final orbit data (igs13385.sp3).



Fig.1 Taiwan Permanent GPS Network

5.1 Performance of CSRF-SINP

In this tested data sets using the processing formulas which described in previous section, about 29.181 km baseline, CSRF was the reference station. Two measuring epochs were necessary for ManGo on-the-fly GPS positioning.

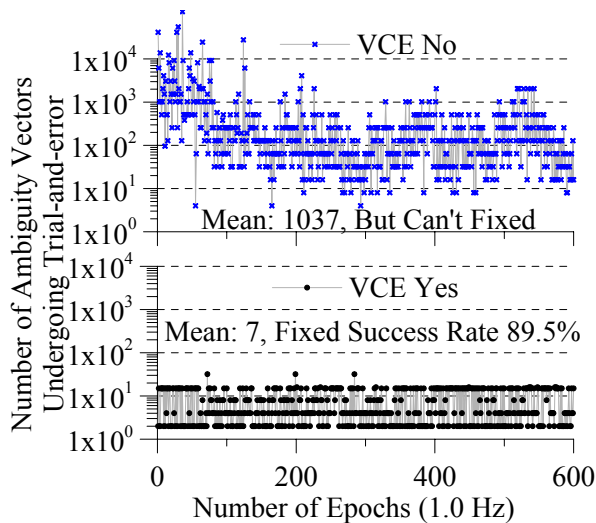


Fig. 2 Trial-and-error vector sets of phase ambiguities for the CSRF-SINP baseline.

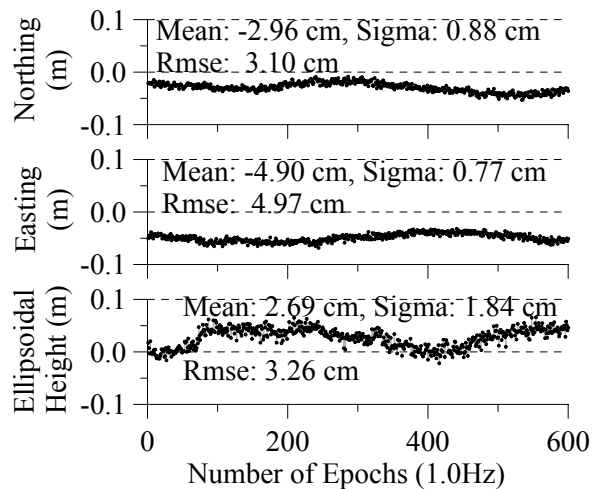


Fig. 3 Relative GPS positioning precision and accuracy for the CSRF-SINP baseline.

The results show that: (i) using the Blues-estimated ambiguity covariance matrix resulting from a propagation of measuring errors contributed to an efficient resolution of the instantaneous epoch ambiguous GPS L1- and L2-carrier phases, easily approaching 90% success rate was obtained, and (ii) the trial-and-error vector sets of integer-valued phase ambiguities with the Blues-estimator yields the rapid and efficient iteration. As shown in Fig. 2, only 7 times of iteration is required when switched-on. In contrast to the case of being switched-off, 1037 times of iteration is required. And (iii) Fig. 3 represents the relative GPS positioning coordinate results. The precision of coordinate and its accuracy are associated with the values of the standard deviation (sigma) and root-mean-square (RMS), respectively. Some remaining tropospheric effects may account the centimeter-level coordinate RMS values, particularly 4.97 cm in easting. Fig. 4 represents the estimated pseudorange and carrier-phase

variance components are displayed (ensemble average in standard deviation are 9.74 and 11.22 m for the pseudoranges, and 0.192 and 0.248 m for the carrier phases, respectively). They needed an average of three times iterations. The Blues-scaled variances are numerically different from epoch to epoch.

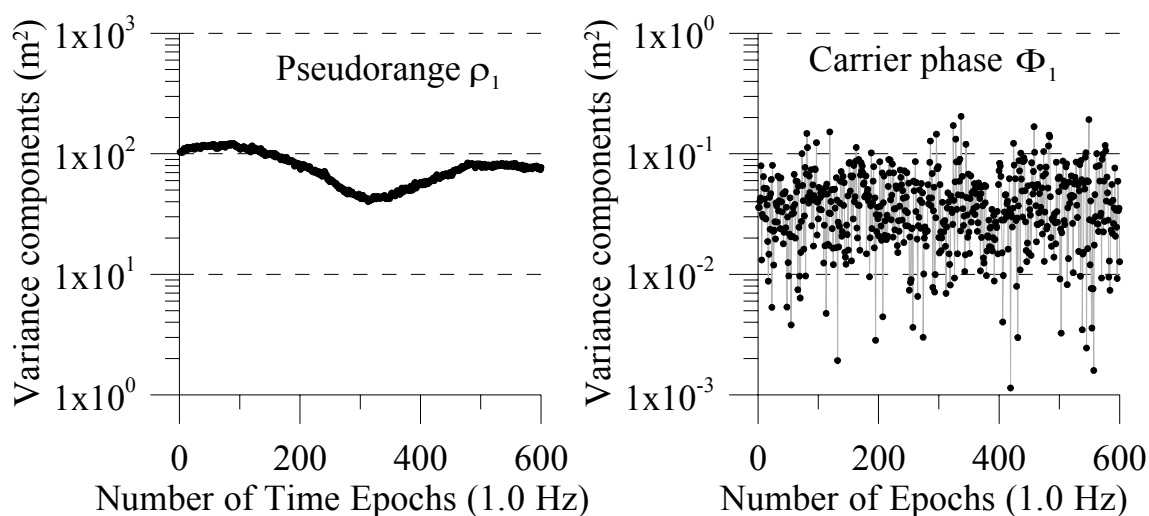


Fig. 4 Pseudorange and carrier-phase variance components estimated with respect to each independent measurement epoch for the CSRFB-SINP baseline.

5.2 Performance of CSRFB-LANY

The second data sets test using the same processed formulas, about 29.613 km baseline, CSRFB was the reference station. The results show that precision and accuracy are as good as the CSRFB-SINP baseline: (i) an efficient resolution of the instantaneous epoch ambiguous GPS L1- and L2-carrier phases, and approaching 90.3% success rate were obtained, and (ii) the trial-and-error vector sets of integer-valued phase ambiguities with the Blues-estimator yields rapid and efficiently iteration. As like shown of Fig. 2, only 6 times of iteration is required when switched-on. In contrast to that of switch-off, 21 times of iteration is required. and (iii) the estimated pseudorange and carrier-phase variance components are displayed(ensemble average in standard deviation are 4.27 and 5.47 m for the pseudoranges, and 0.207 and 0.265 m for the carrier phases, respectively). Fig. 5 represents the relative GPS positioning coordinate results.

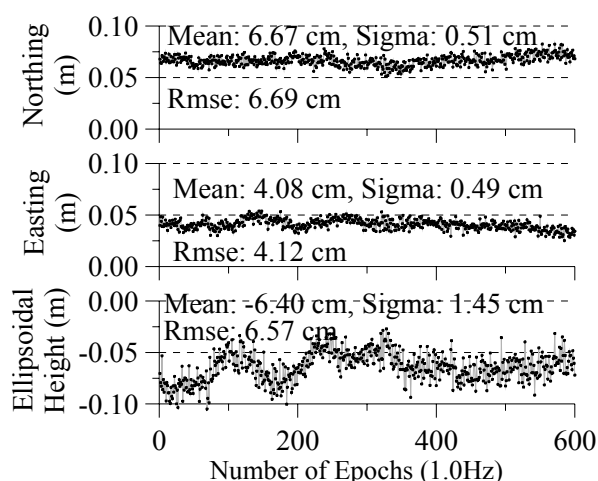


Fig. 5 Relative GPS positioning precision and accuracy for the CSRFB-LANY baseline.

5.3 Performance Comparison of LANY-SINP

The third tested data sets using the same processed formulas, about 54.508 km baseline, LANY was reference stations. The results show in Fig. 6 that ambiguity-fixed position solution only approaching 70% success rate was obtained that using the two-epoch data. If using the multi-epoch data processing exceeded a maximum of six epochs, the set was noted as a failure in ambiguity resolution. A 90% success rate was obtained. The coordinate results are exemplified in Fig. 7, where a distinction between the ambiguity-fixed and ambiguity-float processing schemes is also made. The ambiguity-fixed position solution is better in precision than the float solution. Some remaining tropospheric and ionospheric effects may account for

the decimeter-level coordinate values, particularly -14.5 cm in northing bias.

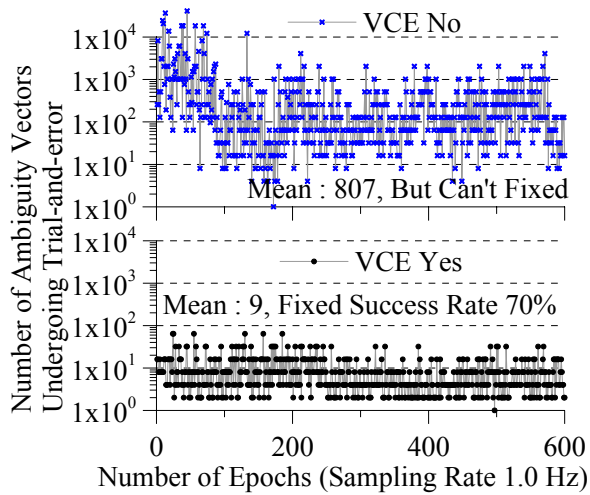


Fig. 6 Trial-and-error vector sets of phase ambiguities for the LANY-SINP baseline.

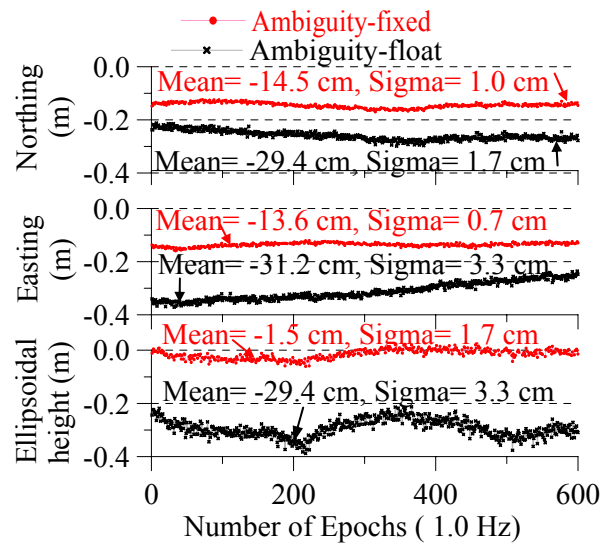


Fig. 7 Relative GPS positioning precision and accuracy for the LANY-SINP baseline.

6. CONCLUSIONS

In this paper, a new rapid approach processing can be determination for the Phase Ambiguity Resolution. Plus the 5th formula can be helpful to estimate the ionosphere effect as a function of time interval and baseline length. A powerful stochastic estimator of the variance-component is developed and incorporated into the algorithm. The volume-preserving and integer-valued transformation techniques are the essential modules of the ManGo software. According to the tests that the Blues-estimated ambiguity covariance matrix resulting from a propagation of measured errors contributed to an efficient resolution of two-epoch ambiguous GPS L1- and L2-carrier phases, the 90% success rate could be obtained for 29 km baselines. They function well as a powerful tool in ambiguity resolution.

When coping with 55 km length baselines, the situation becomes complicated due to sporadic multipath anomaly, ionospheric scintillation and physical correlation between measurements. At that time, the processing is unable to define their proper expressions. So that, improved the double-difference combination of ranging measurements is required on the modeling errors such as residual tropospheric delays by using the precise atmospheric data.

REFERENCES:

- Goad C. C. and Yang, M. (1997). "A new approach to precision airborne GPS positioning for photogrammetry," *Photogrammetric Engineering & Remote Sensing*, Vol. 63, No. 9, pp. 1067-1077.
- Mohamed, A. H., and Schwarz, K. P. (1998). "A simple and economical algorithm for GPS ambiguity resolution on the fly using whitening filter." *Navigation*, Vol. 45, No. 3, pp. 221-231.
- Teunissen, P. J. G., de Jonge, P. J., and Tiberius, C. C. J. M., 1997, "Performance of the LAMBDA Method for Fast GPS Ambiguity Resolution," *Navigation*, Vol. 44, No. 3, pp. 373-383.
- Wu, J., and Yeh, T. F. (2005). "Single-epoch weighting adjustment of GPS phase observables." *Navigation*, Vol. 52, No. 1, pp. 39-47.